



**HAL**  
open science

## Tightrope bubbles

Hélène de Maleprade, Matthias Pautard, Christophe Clanet, David Quéré

► **To cite this version:**

Hélène de Maleprade, Matthias Pautard, Christophe Clanet, David Quéré. Tightrope bubbles. *Applied Physics Letters*, 2019, 114, 10.1063/1.5102148 . hal-02173051

**HAL Id: hal-02173051**

**<https://hal.sorbonne-universite.fr/hal-02173051v1>**

Submitted on 4 Jul 2019

**HAL** is a multi-disciplinary open access archive for the deposit and dissemination of scientific research documents, whether they are published or not. The documents may come from teaching and research institutions in France or abroad, or from public or private research centers.

L'archive ouverte pluridisciplinaire **HAL**, est destinée au dépôt et à la diffusion de documents scientifiques de niveau recherche, publiés ou non, émanant des établissements d'enseignement et de recherche français ou étrangers, des laboratoires publics ou privés.


# Tightrope bubbles

Cite as: Appl. Phys. Lett. **114**, 233704 (2019); <https://doi.org/10.1063/1.5102148>

Submitted: 24 April 2019 . Accepted: 19 May 2019 . Published Online: 13 June 2019

Hélène de Maleprade , Matthias Pautard , Christophe Clanet, and David Quéré

## COLLECTIONS

 This paper was selected as Featured



View Online



Export Citation



CrossMark

## ARTICLES YOU MAY BE INTERESTED IN

[Nanotesla sensitivity magnetic field sensing using a compact diamond nitrogen-vacancy magnetometer](#)

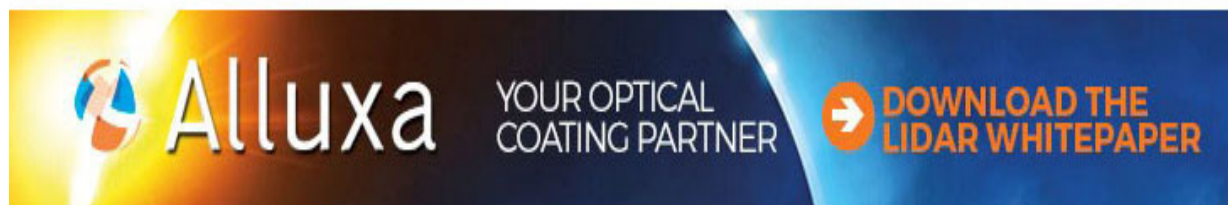
Applied Physics Letters **114**, 231103 (2019); <https://doi.org/10.1063/1.5095241>



[Dual-polarization analog optical phase conjugation for focusing light through scattering media](#)

Applied Physics Letters **114**, 231104 (2019); <https://doi.org/10.1063/1.5097181>

[A call to service](#)

Applied Physics Letters **114**, 230401 (2019); <https://doi.org/10.1063/1.5111857>



 **Alluxa** YOUR OPTICAL COATING PARTNER  **DOWNLOAD THE LIDAR WHITEPAPER**

# Tightrope bubbles



Cite as: Appl. Phys. Lett. **114**, 233704 (2019); doi: 10.1063/1.5102148

Submitted: 24 April 2019 · Accepted: 19 May 2019 ·

Published Online: 13 June 2019



View Online



Export Citation



CrossMark

Hélène de Maleprade, Matthias Pautard, Christophe Clanet, and David Quéré<sup>a)</sup>

## AFFILIATIONS

Physique & Mécanique des Milieux Hétérogènes, UMR 7636 du CNRS, ESPCI Paris, PSL Research University, 75005 Paris, France and LadHyX, UMR 7646 du CNRS, École polytechnique, 91128 Palaiseau, France

<sup>a)</sup> Author to whom correspondence should be addressed: [david.quere@espci.fr](mailto:david.quere@espci.fr)

## ABSTRACT

Droplets moving along fibers have a mobility limited by viscous dissipation. Here, we discuss the opposite situation of bubbles moving on threads immersed in water. Contrasting with drops, the mobility is generally fixed by a visco-inertial skin friction, which allows them to move at much larger velocity than reported in the dual situation. We conclude by establishing how the friction becomes purely viscous when increasing the bath viscosity.

Published under license by AIP Publishing. <https://doi.org/10.1063/1.5102148>

Aerophilic materials, by definition, remain dry when immersed in water. A few insects (such as *Notonecta*) or spiders (such as *Argyroneta Aquatica*) have a textured, aerophilic body covered by a plastron of air, which enables them to breathe and survive under water.<sup>1,2</sup> Air spreads very fast on immersed aerophilic solids, with typical velocities as high as 1 m/s.<sup>3,4</sup> However, the spreading may be frustrated if the surface is not flat.<sup>5</sup> For instance, air on an immersed aerophilic thread will form a bubble coexisting with a film of air trapped in the texture. When the thread is tilted, the bubble starts moving along it under the action of buoyancy, contrasting with other kinds of threads for which contact angle hysteresis pins the bubbles.<sup>6</sup> Hence, such a device allows us to guide air through water in a controlled way. In this paper, we characterize the mobility of air bubbles moving along immersed, tilted, aerophilic fibers.

Fibers are polyamide threads with radius ranging from 100  $\mu\text{m}$  to 200  $\mu\text{m}$ . They are made aerophilic using a commercial spray (Ultra Ever Dry, UltraTech International), consisting of a suspension of hydrophobic nanoparticles dispersed in acetone. Up to three spray treatments are applied to ensure a good coverage of the fiber, each operation being followed by 15 min of drying. Advancing and receding contact angles of air on a similar flat surface immersed in water are  $21^\circ \pm 1^\circ$  and  $14^\circ \pm 4^\circ$ , respectively, showing the combination of the low contact angle and low hysteresis characteristic of an aerophilic state.<sup>4,7</sup> Once immersed into a tank of water or water-glycerol mixture (density  $\rho$  and viscosity  $\eta$ ), these fibers remain covered by a thin layer of air—a phenomenon we attribute to the low value of the receding contact angle that prevents air from dewetting the fiber. The experiment consists in capturing millimeter-size air bubbles on such tilted fibers and in observing the resulting motion. Bubbles (volume  $\Omega$ ) are

dispensed from syringes filled with air and immersed in the tank, 1 cm below the thread. Observations are made from side movies shot at 200 frames per second, using a high-speed video camera (Phantom Miro M310).

After being released, a bubble rises vertically until it reaches a thread tilted by an angle  $\alpha$  to the horizontal. As seen in the chronophotography displayed in Fig. 1 and in the supplementary material, the buoyant bubble moves along the fiber after its capture. Fibers being covered by a thin plastron of air, there is no apparent additional air deposition during the rise so that the motion takes place at a constant volume  $\Omega$ . The bubble being much larger than the fiber radius, it has a nonaxisymmetric shape, similar to that of a large wetting drop hanging from a thin thread.<sup>8,9</sup> The interval between successive pictures is constant (and equal to 40 ms), which evidences the constant velocity  $V$  of the bubble reached after typically 100 ms, and equal to  $11.0 \pm 0.2$  cm/s in this experiment.

In such a stationary regime, the bubble dynamics results from a balance between the buoyancy force  $\rho\Omega g \sin \alpha$  and some velocity-dependent friction, which we try to characterize. To that end, we vary the tilt angle  $\alpha$  and measure the velocity  $V$  for each tilt, which directly yields the relationship between force and velocity—a crucial information for establishing the friction law. Such a plot is displayed in Fig. 2(a), where bubble speeds are observed to be of order 10 cm/s, that is, 10 times larger than that of a nonviscous drop with similar volume rolling down along a tilted fiber,<sup>10</sup> which reveals strong differences in the dissipation mechanism. Indeed, the scaling law observed between the force and the velocity is not usual (in the context of interfacial dynamics) since data follow a line of slope  $1.50 \pm 0.05$ , close to  $3/2$ , on the logarithmic scales of

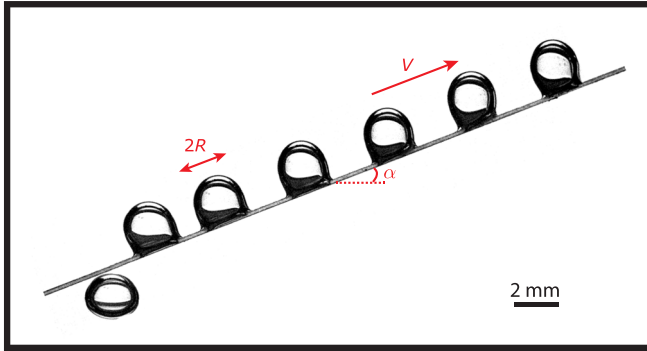


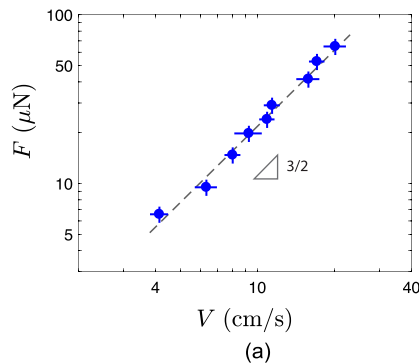
**FIG. 1.** Chronophotography of an air bubble with volume  $\Omega \approx 8.2 \mu\text{l}$  captured by a fiber with a radius of  $115 \mu\text{m}$  tilted by  $\alpha = 21^\circ$ . The time between two successive images is 40 ms. The motion after typically 100 ms is observed to take place at a constant velocity  $V \approx 11 \text{ cm/s}$ .

**Fig. 2(a)**—which differs from both the linear and quadratic relationships expected for viscous and inertial frictions.<sup>3,10</sup>

Contrasting with the case of drops for which dissipation happens close to the contact line,<sup>9,10</sup> air bubbles are not viscous enough to generate inner friction. Hence, we rather expect dissipation to occur mainly in the surrounding water. For  $R \approx 1 \text{ mm}$  and  $V \approx 10 \text{ cm/s}$ , the typical Reynolds number  $Re = \rho VR/\eta$  in water is  $\sim 100$ , suggesting a visco-inertial scenario for the friction. We assume a no-slip boundary condition at the air/water interface, which can first be seen as a consequence of the contrast of viscosity between air and water. But other factors can contribute to rigidify the bubble surface: nanobeads detached from the aerophilic coating can get adsorbed at the interface,<sup>11,12</sup> and surfactants can also be present and further reinforce the air/water surface.

The resulting skin friction develops over the thickness  $\delta$  of the viscous boundary layer around the rising bubble, that is,  $\delta \approx \sqrt{\nu R/V}$ , where  $\nu = \eta/\rho$  is the kinematic viscosity of the liquid. This formula provides  $\delta \approx 0.1 \text{ mm}$ , that is, about 10% of the bubble size, in agreement with the hypothesis of a visco-inertial friction. The corresponding friction  $F \approx \eta R^2 V/\delta$  can thus be written as

$$F \approx \sqrt{\rho\eta}(RV)^{3/2}. \tag{1}$$



We recover the  $V^{3/2}$ -dependency observed in **Fig. 2(a)**. Balancing this expression with buoyancy provides the terminal velocity  $V$ ,

$$V \approx \left( \frac{g^2 \sin^2 \alpha}{\nu} \right)^{1/3} R. \tag{2}$$

This law predicts typical velocities of 10 cm/s for millimetric bubbles rising in water on a fiber inclined by a few degrees, in excellent agreement with the data displayed in **Fig. 2(a)**. The terminal velocity is linear in drop size  $R$ , and it is predicted to be a slowly decreasing function of the bath kinematic viscosity, characterized by an exponent  $-1/3$ , that is, between 0 (inertial friction) and  $-1$  (viscous friction).

Using water-glycerol mixtures, we can test how the speed  $V$  depends on  $\nu$ . As reported in **Fig. 2(b)**,  $V$  is indeed found to decrease as  $\nu^{-1/3}$  [Eq. (2)], up to  $\nu^* = 30 \text{ mm}^2/\text{s}$ , above which it decreases as  $\nu^{-1}$ . At the transition  $\nu^*$ , the boundary layer thickness  $\delta$  becomes comparable to the bubble size  $R \approx 1 \text{ mm}$ , which happens at a Reynolds number of order 1. This can be further verified by substituting Eq. (2) in the definition of the Reynolds number  $Re$ , which yields  $\nu^* = R^{3/2} g^{1/2} \sin^{1/2} \alpha$  for  $Re \approx 1$ . For a millimetric bubble and an angle  $\alpha$  of a few degrees, we get  $\nu^* \approx 50 \text{ mm}^2/\text{s}$ , in good agreement with the value of  $\nu^*$  in **Fig. 2(b)**. Above  $\nu^*$ , a Stokes friction  $F = 6\pi\eta VR$  develops around the quasi-spherical bubble (assuming again a no-slip condition at the bubble surface). Balancing it with buoyancy, we obtain the classical law of sedimentation

$$V = \frac{2 R^2 g \sin \alpha}{9 \nu}. \tag{3}$$

The second dashed line in **Fig. 2(b)** shows Eq. (3), where it is observed to be in excellent agreement with our data, without any fitting coefficient.

In summary, an aerophilic fiber is able to capture and to guide air bubbles. At low bath viscosity, a skin friction develops around the rising bubble, leading to a nonlinear friction force varying as the terminal velocity to 3/2. This regime is very different from that for a drop, where dissipation happens inside, mainly in the liquid corners that end it. Here, bubbles totally wet the fiber, and the dissipation in the air corners is negligible, which explains that friction mainly arises from the surrounding liquid. At larger bath viscosity, typically around 50

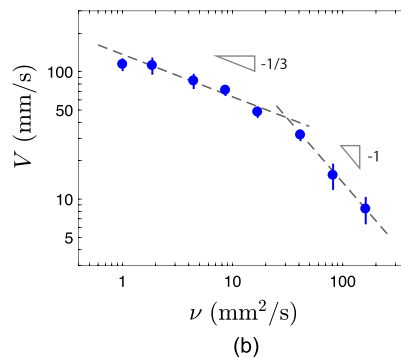


**FIG. 2.** (a) Friction force  $F$  as a function of the bubble terminal velocity  $V$ , for bubbles with  $\Omega = 8.2 \mu\text{l}$  and a fiber radius  $190 \mu\text{m}$ . The dashed line shows the slope 3/2 expected from Eq. (1), adjusted by a numerical coefficient 16. Each point is the result of 4 or 5 experiments. (b) Terminal velocity  $V$  as a function of the kinematic viscosity  $\nu$  of the water-glycerol mixture in the tank, for bubbles with  $\Omega = 9.5 \mu\text{l}$  and a fiber with a radius of  $150 \mu\text{m}$ , tilted by  $\alpha = 21^\circ$ . Dashed lines successively show the slope  $-1/3$  of Eq. (2) adjusted with a numerical coefficient 0.5 and Eq. (3) and its slope  $-1$ . Each point is the result of 4 or 5 experiments.

times more viscous than water, the friction force turns into a Stokes friction, linear in velocity. Inertial regimes might occur for larger volumes (since it appears difficult to reduce the bath viscosity), but larger bubbles will often detach from the fiber: this limits the characterization of the phenomenon to the regimes we explored.

See the [supplementary material](#) for the movie that corresponds to Fig. 1, where we can see an air bubble with a volume of  $8.2 \mu\text{l}$  captured by an aerophilic thread (radius:  $115 \mu\text{m}$ ), tilted by  $21^\circ$ . The video-camera is tilted by the same angle. The video is slowed down 10 times, and the bubble quickly reaches a stationary velocity of about  $140 \text{ mm/s}$ .

## REFERENCES

- <sup>1</sup>P. Ditsche-Kuru, E. S. Schneider, J. E. Melskotte, M. Brede, A. Leder, and W. Barthlott, "Superhydrophobic surfaces of the water bug *notonecta glauca*: A model for friction reduction and air retention," *Beilstein J. Nanotechnol.* **2**, 137–144 (2011).
- <sup>2</sup>N. J. Shirtcliffe, G. McHale, M. I. Newton, C. C. Perry, and F. B. Pyatt, "Plastron properties of a superhydrophobic surface," *Appl. Phys. Lett.* **89**, 104106 (2006).
- <sup>3</sup>J. Wang, Y. Zeng, F. Q. Nie, J. Zhai, and L. Jiang, "Air bubble bursting effect of lotus leaf," *Langmuir* **25**, 14129–14134 (2009).
- <sup>4</sup>H. de Maleprade, C. Clanet, and D. Quéré, "Spreading of bubbles after contacting the lower side of an aerophilic slide immersed in water," *Phys. Rev. Lett.* **117**, 094501 (2016).
- <sup>5</sup>B. J. Carroll, "The accurate measurement of contact angle, phase contact areas drop volume, and Laplace excess pressure in drop-on-fiber systems," *J. Colloid Interface Sci.* **57**, 488–495 (1976).
- <sup>6</sup>C. Yu, M. Cao, Z. Dong, K. Li, C. Yu, J. Wang, and L. Jiang, "Aerophilic electrode with cone shape for continuous generation and efficient collection of  $\text{H}_2$  bubbles," *Adv. Funct. Mater.* **26**, 6830–6835 (2016).
- <sup>7</sup>A. B. D. Cassie, "Contact angles," *Discuss. Faraday Soc.* **3**, 11–16 (1948).
- <sup>8</sup>G. McHale and M. I. Newton, "Global geometry and the equilibrium shapes of liquid drops on fibers," *Colloids Surf., A* **206**, 79–86 (2002).
- <sup>9</sup>É. Lorenceau, C. Clanet, and D. Quéré, "Capturing drops with a thin fiber," *J. Colloid Interface Sci.* **279**, 192–197 (2004).
- <sup>10</sup>T. Gilet, D. Terwagne, and N. Vandewalle, "Droplets sliding on fibers," *Eur. Phys. J. E* **31**, 253–262 (2010).
- <sup>11</sup>F. J. Peaudecerf, J. R. Landel, R. E. Goldstein, and P. Luzzatto-Fegiz, "Traces of surfactants can severely limit the drag reduction of superhydrophobic surfaces," *Proc. Natl. Acad. Sci. U.S.A.* **114**, 7254–7259 (2017).
- <sup>12</sup>A. Gaddam, A. Agrawal, S. S. Joshi, and M. C. Thompson, "Slippage on a particle-laden liquid-gas interface in textured microchannels," *Phys. Fluids* **30**, 032101 (2018).